POLITECNICO DI TORINO
Repository ISTITUZIONALE

Fredholm factorization of Wiener-Hopf scalar and matrix kernels

Original
Fredholm factorization of Wiener-Hopf scalar and matrix kernels / Daniele, V., Lombardi, G.. - In: RADIO SCIENCE. - ISSN 0048-6604. - STAMPA. - 42:RS6S01(2007), pp. 1-19. [10.1029/2007RS003673]

Availability:
This version is available at: 11583/1662347 since:

Publisher:
American Geophysical Union

Published
DOI:10.1029/2007RS003673

Terms of use:

This article is made available under terms and conditions as specified in the corresponding bibliographic description in the repository

Publisher copyright

(Article begins on next page)

14 October 2026

Fredholm factorization of Wiener-Hopf scalar and matrix kernels

V. Daniele[1,2] and G. Lombardi[1]

Received 18 April 2007; revised 23 July 2007; accepted 13 August 2007; published 24 November 2007.

[1] A general theory to factorize the Wiener-Hopf (W-H) kernel using Fredholm Integral Equations (FIE) of the second kind is presented. This technique, hereafter called Fredholm factorization, factorizes the W-H kernel using simple numerical quadrature. W-H kernels can be either of scalar form or of matrix form with arbitrary dimensions. The kernel spectrum can be continuous (with branch points), discrete (with poles), or mixed (with branch points and poles). In order to validate the proposed method, rational matrix kernels in particular are studied since they admit exact closed form factorization. In the appendix a new analytical method to factorize rational matrix kernels is also described. The Fredholm factorization is discussed in detail, supplying several numerical tests. Physical aspects are also illustrated in the framework of scattering problems: in particular, diffraction problems. Mathematical proofs are reported in the paper.

Citation: Daniele, V., and G. Lombardi (2007), Fredholm factorization of Wiener-Hopf scalar and matrix kernels, *Radio Sci.*, *42*, RS6S01, doi:10.1029/2007RS003673.

1. Introduction

[2] The Wiener-Hopf (W-H) method is a general analytical technique which is able to deal with different kind of mathematical-physical and/or engineering problems [*Noble*, 1988; *Weinstein*, 1969; *Daniele*, 2003, 2004]. According to the authors' opinion the Wiener-Hopf method is one of the most important mathematical tool to obtain closed form solutions for a consistent number of fundamental (canonical) problems.

[3] In application problems, the W-H technique deals with the solution of the functional equation defined in the complex α plane:

$$G(\alpha)F_+(\alpha) = F^s_-(\alpha) + \frac{R}{\alpha - \alpha_o} = F_-(\alpha) \qquad (1)$$

This equation is called the Wiener-Hopf equation and it can be classified as scalar or vector, by respectively involving scalar quantities ($F_+(\alpha)$, R, $F^s_-(\alpha)$, $F_-(\alpha)$ and $G(\alpha)$) or n-dimensional vector quantities ($F_+(\alpha)$, R, $F^s_-(\alpha)$ and $F_-(\alpha)$) and matrix quantities of order n ($G(\alpha)$).

[4] The unknowns of equation (1) are the plus and the minus functions $F_+(\alpha)$ and $F^s_-(\alpha)$. The functions $F_+(\alpha)$ and $F_-(\alpha)$ are generally Laplace transforms and they vanish as $\alpha \to \infty$.

$$F_+(\alpha) = \int_0^\infty f(z)e^{j\alpha z}dz$$
$$F_-(\alpha) = \int_{-\infty}^0 f(z)e^{j\alpha z}dz \qquad (2)$$

The plus and the minus functions are called standard if they are regular respectively in the upper half plane $Im[\alpha] \geq 0$ and in the lower half plane $Im[\alpha] \leq 0$.

[5] The function $G(\alpha)$ is called kernel of the W-H equation. Note that the $G(\alpha)$ and its inverse ($G^{-1}(\alpha) = [G(\alpha)]^{-1}$) are regular function in the real axis $Im[\alpha] = 0$. The kernel is defined by the physical problem; therefore it is known together with R and α_o. R and α_o are related to the source, it is always supposed that $Im[\alpha_o] \neq 0$. The properties of the problem are defined by the spectrum of $G(\alpha)$. We assume the absence of essential singularities in the spectrum, except at the infinity. The zeroes of det[G(α)] and det[$G^{-1}(\alpha)$] define the structural singularities. We observe that the branch point singularities define the continuous spectrum and the poles define the discrete spectrum.

[6] Although (1) presents two unknowns, $F_+(\alpha)$ and $F^s_-(\alpha)$, the Wiener-Hopf equation constitute a closed mathematical problem which yields proper solution without any additional information, see proofs of the existence and the uniqueness of the solution in the

[1]Dipartimento di Elettronica, Politecnico di Torino, Torino, Italy.
[2]Also at Istituto Superiore Mario Boella (ISMB), Torino, Italy.

Copyright 2007 by the American Geophysical Union.
0048-6604/07/2007RS003673

classical mathematical literature [*Gohberg and Krein*, 1960].

[7] The W-H technique yields the following solution of the equation (1) [*Noble*, 1988; *Daniele*, 2004]:

$$F_+(\alpha) = G_+^{-1}(\alpha)G_-^{-1}(\alpha_o)\frac{R}{\alpha-\alpha_o} = G_+^{-1}(\alpha)G_+(\alpha_o)G^{-1}(\alpha_o)\frac{R}{\alpha-\alpha_o} \quad (3)$$

$$F_-(\alpha) = F_-^s(\alpha) + \frac{R}{\alpha-\alpha_o} = G_-(\alpha)G_-^{-1}(\alpha_o)\frac{R}{\alpha-\alpha_o} \quad (4)$$

where $G_+^{-1}(\alpha) = [G_+(\alpha)]^{-1}$ and $G_-^{-1}(\alpha) = [G_-(\alpha)]^{-1}$ arise from the factorization of the kernel $G(\alpha)$:

$$G(\alpha) = G_-(\alpha)G_+(\alpha) \quad (5)$$

[8] In (3) and (4) the factorized function $G_+(\alpha)$ and $G_-(\alpha)$ and their inverses $G_+^{-1}(\alpha)$ and $G_-^{-1}(\alpha)$ are regular respectively in the half planes $Im[\alpha] \geq 0$ and $Im[\alpha] \leq 0$ and present algebraic behavior as $\alpha \to \infty$. The solution (3)–(4) shows that the central problem for the solution of Wiener-Hopf equation (1) is the factorization of the kernel (5). The simplest class of W-H equations are the scalar ones where closed form solutions are always possible [*Noble*, 1988; *Weinstein*, 1969; *Daniele*, 2004]. Conversely the general solution for vector W-H equations is not available in closed form and only some progress has been done to develop a general method of explicit solution [*Daniele*, 2004; *Hashimoto et al.*, 1993].

[9] Today we are able to factorize in closed form triangular matrices, rational matrices, i.e., matrices with entries that are rational functions of α, and matrices that commute with rational matrices [*Daniele*, 1984, 2004]. The need of developing an approximate technique of factorization arises from all the cases where no explicit factorization is possible.

[10] Several powerful mathematical methods of functional analysis help to efficiently solve W-H problems, for instance: iterative methods, moment methods, regularization methods and so on.

[11] Furthermore, since it is possible to factorize rational matrices in closed form, the vector factorization problem can be approximated by introducing rational approximants (for instance Padé type [*Abrahams*, 2000]) for the entries of the matrix kernel. We have investigated this technique in practical engineering applications [see *Daniele*, 2004].

[12] We are convinced that the reduction to Fredholm equations is possibly the best way to face the factorization problems.

[13] We confide in the Fredholm method since we experienced its efficacy and efficiency in different problems using different quadratures. Conversely the Padé approximants (or more in general rational approximants) do not assure accuracy/convergency when the order of the rational representation is increased.

[14] The aim of this paper is to present an efficient method to solve a general W-H problem which is based on the reduction of the factorization problem to the solution of a Fredholm equation of the second kind.

[15] This paper is organized as follow. In section 2 we derive the factorization of kernel using an homogeneous W-H formulation. Section 3 and 4 shows respectively the reduction of the W-H equations to Fredholm integral equations and their numerical solution. Section 4 includes some tools to improve the convergence of Fredholm integral equations and details on the analytical continuation of the numerical solution. Section 5 validates the proposed technique, presenting several numerical tests with kernel of practical applications. This section presents the efficiency and the convergence of the approximate Fredholm solution in particular in the framework of scattering/diffraction problems. See *Gohberg and Krupnik* [1992] and *Jones* [1979] for proofs on the compactness of kernel for Fredholm integral equations derived from W-H problems.

2. Kernel Factorization Using Homogeneous W-H Formulation

[16] In order to factorize a matrix kernel $G(\alpha)$, let us introduce the homogeneous W-H equation [*Vekua*, 1967]:

$$G(\alpha)U_{i+}(\alpha) = U_{i-}(\alpha) \quad (6)$$

where the plus function $U_{i+}(\alpha)$ and the minus function $U_{i-}(\alpha)$ are not Laplace transforms, but such that the quantities $\frac{U_{i+,-}(\alpha)}{\alpha}$ vanish as $\alpha \to \infty$. Using n independent solutions of (6) $\{U_{i+}(\alpha), U_{i-}(\alpha)\}$ with $i = 1.n$, we obtain the factorized matrices of $G(\alpha)$:

$$\begin{cases} G_-(\alpha) = |U_{1-}(\alpha), U_{2-}(\alpha), .., U_{n-}(\alpha)| \\ G_+(\alpha) = |U_{1+}(\alpha), U_{2+}(\alpha), .., U_{n+}(\alpha)|^{-1} \end{cases} \quad (7)$$

To get n independent solutions of (6) we introduce new auxiliary unknowns which are Laplace transforms:

$$X_{i+}(\alpha) = \frac{U_{i+}(\alpha)}{\alpha-\alpha_p} \quad (8)$$

where α_p is an arbitrary point with negative imaginary part ($Im[\alpha_p] < 0$). In the following we suppose that α_p does not belong to the null space of $G(\alpha)$ and $G^{-1}(\alpha)$:

$$Null[G(\alpha)] = \{\alpha : \det[\mathrm{G}](\alpha) = 0\} \tag{9}$$

$$Null\left[G^{-1}(\alpha)\right] = \left\{\alpha : \det\left[\mathrm{G}^{-1}\right](\alpha) = 0\right\} \tag{10}$$

Note that if $\overline{\alpha} \in Null[G(\alpha)]$ then $U_{i-}(\overline{\alpha}) = 0$ and if $\overline{\alpha} \in Null[G^{-1}(\alpha)]$ then $U_{i+}(\overline{\alpha}) = 0$.

[17] From (6)–(8) we obtain:

$$G(\alpha)X_{i+}(\alpha) = \frac{U_{i-}(\alpha)}{\alpha - \alpha_p} \tag{11}$$

where the unknowns $X_{i+}(\alpha)$ and $\frac{U_{i-}(\alpha)}{\alpha-\alpha_p}$ vanish as $\alpha \to \infty$. Equation (11) can be rewritten as:

$$G(\alpha)X_{i+}(\alpha) = \frac{U_{i-}(\alpha) - U_{i-}(\alpha_p)}{\alpha - \alpha_p} + \frac{U_{i-}(\alpha_p)}{\alpha - \alpha_p} \tag{12}$$

[18] We assume $U_{i-}(\alpha_p) = R_i$ with $i = 1.n$ where R_i is the canonical basis for the n-dimensional space.

[19] From (12) we obtain n independent solutions $U_{i+}(\alpha) = (\alpha - \alpha_p)\, X_{i+}(\alpha)$ that provide the factorized matrix $G_+(\alpha)$ using (7). We observe that vectors $U_{i+}(\alpha)$ depend on the choice of α_p; therefore we use the notation $G_+(\alpha, \alpha_p)$ instead of $G_+(\alpha)$ for the factorized matrix when we want to focus the dependence on α_p. From (3)–(5) we note that the factorized matrix $G_+(\alpha)$ can be defined up to a multiplicative constant matrix. In the following we show that the change of α_p on the evaluation of $G_+(\alpha)$ yields different $G_+(\alpha, \alpha_p)$ matrices which differ from each other up to a premultiplicative constant matrix.

[20] Let us introduce the factorized matrices $G_{+,-}(\alpha)$, $G_+(\alpha, \alpha_1)$ and $G_+(\alpha, \alpha_2)$ where $G_{+,-}(\alpha)$ are arbitrary factorized matrices of $G(\alpha)$ and, $G_+(\alpha, \alpha_1)$ and $G_+(\alpha, \alpha_2)$ are determined by the W-H equation with different α_p values: α_1 and α_2. From (12) we obtain the vectors $X^1_{i+}(\alpha)$ and $X^2_{i+}(\alpha)$ respectively for $\alpha_p = \alpha_1$ and $\alpha_p = \alpha_2$:

$$X^{1,2}_{i+}(\alpha) = \frac{G_+^{-1}(\alpha)G_-^{-1}(\alpha_{1,2})}{\alpha - \alpha_{1,2}} R_i \tag{13}$$

From (7)–(8) and (13) we obtain the expression of $G_+(\alpha, \alpha_1)$ and $G_+(\alpha, \alpha_2)$ and it yields:

$$G_+(\alpha, \alpha_2) = K\, G_+(\alpha, \alpha_1) \tag{14}$$

where the constant matrix K is obtained after some algebraic manipulation and is given by:

$$K = \left|G_-^{-1}(\alpha_2)R_1, G_-^{-1}(\alpha_2)R_2, G_-^{-1}(\alpha_2)R_3, .., G_-^{-1}(\alpha_2)R_n\right|^{-1} \cdot \left|G_-^{-1}(\alpha_1)R_1, G_-^{-1}(\alpha_1)R_2, G_-^{-1}(\alpha_1)R_3, .., G_-^{-1}(\alpha_1)R_n\right| \tag{15}$$

In the following we avoid the details on the optimization of α_p in the $Im[\alpha] < 0$ plane. However, we notice that an unsuitable choice of α_p gives an unsatisfactory numerical precision on the evaluation of the factorized matrices using approximate techniques. In fact the use of α_p introduces an apparent singularity, consequently even though it does not produce effects on the analytical closed form solutions, it increases the numerical instability on the approximate numerical solution in the region of the α plane close to α_p. In order to avoid this problem we suggest to define α_p in the context of a physical problem. For instance in scattering problems with open structures a physical source is constituted by a plane wave that yields a source term with a pole in the α plane. In this context we suggest to assume α_p in the region where the source pole is located.

3. Reduction of the Wiener-Hopf Equation to Fredholm Integral Equation

[21] As the Riemann-Hilbert problem [*Vekua*, 1967], the Wiener-Hopf equations can be formulated in terms of Fredholm integral equations. Let us consider equation (1) and integrate it on the $\gamma_{1,2}$ indented contours (see Figure 1). Three different cases are discriminated in terms of $Im[\alpha_o]$:

3.1. Case A: $Im[\alpha_o] < 0$

[22] We assume standard plus and minus functions in (1) and we close the contour γ_1 with a half ring located in the half plane $Im[\alpha] < 0$ with radius $\rho \to \infty$. By integrating clockwise we obtain:

$$\int_{\gamma_1} \frac{G(u)F_+(u)}{u - \alpha} du - \int_{\gamma_1} \frac{F^s_-(u)}{u - \alpha} du = \int_{\gamma_1} \frac{R}{(u - \alpha_o)(u - \alpha)} du \tag{16}$$

Using the residue formula it yields:

$$\int_{\gamma_1} \frac{G(u)F_+(u)}{u - \alpha} du = 2\pi j \frac{R}{\alpha - \alpha_o} \tag{17}$$

$$\int_{\gamma_1} \frac{F_-^s(u)}{u-\alpha} du = 0 \tag{18}$$

because $F_-(u)$ is regular in the half plane $Im[u] < 0$. Using the γ_2 contour we obtain similarly:

$$\int_{\gamma_2} \frac{F_+(u)}{u-\alpha} du = 0 \tag{19}$$

The integrals defined in (16) and (19) can be written respectively in terms of Cauchy principal value integrals:

$$\int_{\gamma_1} \frac{G(u)F_+(u)}{u-\alpha} du = P.V. \int_{-\infty}^{+\infty} \frac{G(u)F_+(u)}{u-\alpha} du + j\pi G(\alpha)F_+(\alpha) \tag{20}$$

$$\int_{\gamma_2} \frac{F_+(u)}{u-\alpha} du = P.V. \int_{-\infty}^{+\infty} \frac{F_+(u)}{u-\alpha} du - j\pi F_+(\alpha) = 0 \tag{21}$$

We substitute (20) in (16) and multiply the result by $G_-^{-1}(\alpha)$:

$$G^{-1}(\alpha) P.V. \int_{-\infty}^{\infty} \frac{G(u)F_+(u)}{u-\alpha} du + j\pi F_+(\alpha) = 2\pi j\, G^{-1}(\alpha) \frac{R}{\alpha-\alpha_o} \tag{22}$$

Finally, we combine (22) with (21), and we obtain the following Fredholm integral equation that holds in the real axis:

$$F_+(\alpha) + \frac{1}{2\pi j} \int_{-\infty}^{\infty} \frac{[G^{-1}(\alpha)G(u) - \mathbf{1}]F_+(u)}{u-\alpha} du = G^{-1}(\alpha) \frac{R}{\alpha-\alpha_o}, \quad Im[\alpha_o] < 0 \tag{23}$$

where $\mathbf{1}$ is the identity matrix of order n (n is the vector dimension of the unknowns).

3.2. Case B: $Im[\alpha_o] > 0$

[23] A slight modification of the previous procedure yields a similar Fredholm integral equations for $Im[\alpha_o] > 0$:

$$F_+(\alpha) + \frac{1}{2\pi j} \int_{-\infty}^{\infty} \frac{[G^{-1}(\alpha)G(u) - \mathbf{1}]F_+(u)}{u-\alpha} du = G^{-1}(\alpha_o) \frac{R}{\alpha-\alpha_o}, \quad Im[\alpha_o] > 0 \tag{24}$$

In particular we need to consider that the plus unknown $F_+(\alpha)$ is nonstandard: it means that the spectrum of $F_+(\alpha)$ contains the pole α_o located in the upper half plane in addiction to standard singularities of plus function (located in lower half plane).

3.3. Case C: $Im[\alpha_o] = 0$

[24] As we have supposed $Im[\alpha_o] \neq 0$, this case is reported only for the completeness of the discussion. Using the same procedure as in case A, when $Im[\alpha_o] = 0$, we need to consider the presence of a new pole in the real axis: α_o. The $\gamma_{1,2}$ contours need to be indented both

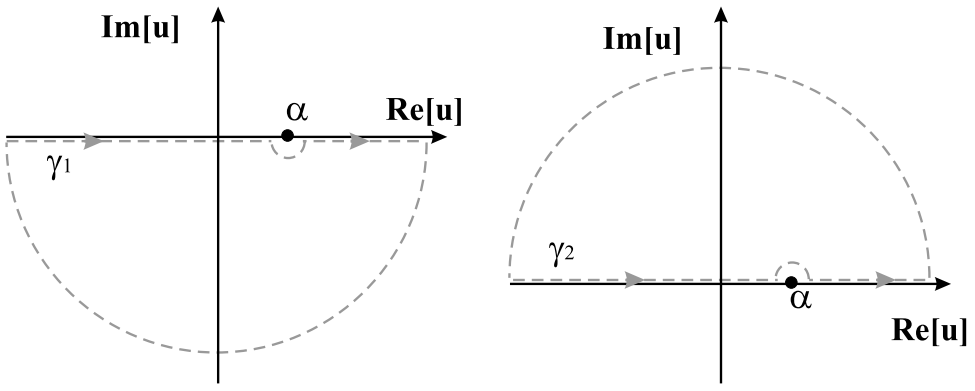

Figure 1. Integration paths for the deduction of the Fredholm integral equation.

near α and α_o. Therefore we obtain the following Fredholm integral equation:

$$F_+(\alpha)+\frac{1}{2\pi j}\int_{-\infty}^{\infty}\frac{[G^{-1}(\alpha)G(u)-\mathbf{1}]F_+(u)}{u-\alpha}du = \frac{1}{2}\frac{G^{-1}(\alpha)R}{\alpha-\alpha_o}+\frac{1}{2}\frac{G^{-1}(\alpha_o)R}{\alpha-\alpha_o} \quad (25)$$

[25] The reduction of W-H equations to Fredholm integral equations is very important for several properties. In particular we observe that efficient techniques are available in literature to obtain approximate solutions of the Fredholm integral equations of second kind [*Kantorovich and Krylov*, 1958]; therefore we must ascertain that the previous integral equations are really of second kind; that is, we state that the kernel $[\frac{G^{-1}(\alpha)G(u)-\mathbf{1}}{u-\alpha}]$ is a compact operator [see *Gohberg and Krupnik*, 1992]. For instance compact operators are those where $G(\alpha)$ and $G^{-1}(\alpha)$ exist and are finite in all the points of the integration line (including the ∞ points) relevant to the Fredholm equation (23)–(25).

3.4. Physical Meaning of the Fredholm Equation in the Framework of Scattering Problems

[26] In the following we show that the integral term

$$\Phi(\alpha)=\int_{-\infty}^{\infty}\frac{[G^{-1}(\alpha)G(u)-\mathbf{1}]F_+(u)}{u-\alpha}du \quad (26)$$

in the Fredholm equations (23), (24), and (25) does not involve the source pole. In fact by assuming:

$$F_+(\alpha)=\frac{T}{\alpha-\alpha_o}+f_r(\alpha) \quad (27)$$

where $f_r(\alpha)$ is regular in α_o, it yields:

$$\frac{1}{2\pi j}\int_{-\infty}^{\infty}\frac{[G(u)-G(\alpha)]T}{(u-\alpha)(u-\alpha_o)}du=\frac{T}{2\pi j(\alpha-\alpha_o)}P.V.\cdot\int_{-\infty}^{\infty}\left[\frac{G(u)-G(\alpha)}{u-\alpha}-\frac{G(u)-G(\alpha_o)}{u-\alpha_o}\right]du+\frac{[G(\alpha_o)-G(\alpha)]T}{2(\alpha-\alpha_o)} \quad (28)$$

where we have used $P.V.\int_{-\infty}^{\infty}\frac{1}{u-\alpha_o}du=\lim_{M\to+\infty}\int_{-M}^{+M}\frac{1}{u-\alpha_o}du=-\pi j$. From (28) we state that the integral function $\Phi(\alpha)$ is regular at $\alpha=\alpha_o$.

[27] In scattering problems with open structures a physical source is typically constituted by a plane wave that yields a source term with a pole in the α plane, that is α_o. Incident and reflected components are related to this pole (geometrical optics component). The integral $\Phi(\alpha)$ generates an extra component whose spectrum does not contain the geometrical optics component. This component is the diffracted field.

4. Numerical Solution of the Fredholm Equations Relevant to W-H Equations

[28] Nowadays general numerical methods for the solution of integral equation are well known in literature. In particular, we recall that the integral equations derived from W-H problems are Fredholm integral equations of second kind. Inhomogeneous Fredholm equations of second kind are usually well conditioned [*Kantorovich and Krylov*, 1958]. Equations (23)–(25) for scattering problems are well conditioned. Efficient techniques to solve these equations are already available in literature: see for example the Nystrom method.

[29] Because of the high convergence rate of equations (23)–(25) we apply a simplified form of discretization. Without loss of generality, let us consider (23) in the following modified form:

$$G(\alpha)F_+(\alpha)+\frac{1}{2\pi j}\int_{-\infty}^{+\infty}\frac{[G(t)-G(\alpha)]F_+(t)}{t-\alpha}dt = \frac{R}{\alpha-\alpha_o},\quad Im[\alpha_o]<0 \quad (29)$$

We discretize (29) using an elementary quadrature scheme:

$$G(\alpha)F_+(\alpha)+\frac{h}{2\pi j}\sum_{i=-A/h}^{A/h}m(\alpha,h\,i)F_+(h\,i)=\frac{R}{\alpha-\alpha_o} \quad (30)$$

where $m(\alpha, t)$ is defined as

$$m(\alpha,t)=\begin{cases}\dfrac{G(t)-G(\alpha)}{t-\alpha}, & t\neq\alpha\\ \dfrac{dG(\alpha)}{d\alpha}, & t=\alpha\end{cases} \quad (31)$$

and the quantities h and $\pm A$ represent respectively the discretization step and the endpoints of the truncated integration interval. By enforcing $\alpha = hr$ with $r = 0, \pm1, \pm2, .., \pm A/h$, (30) becomes the following linear system of equations:

$$G(h\,r)F_+(h\,r)+\frac{h}{2\pi j}\sum_{i=-A/h}^{A/h}m(h\,r,h\,i)F_+(h\,i) = \frac{R}{h\,r-\alpha_o},\quad r=0,\pm1,\pm2,..\pm\frac{A}{h} \quad (32)$$

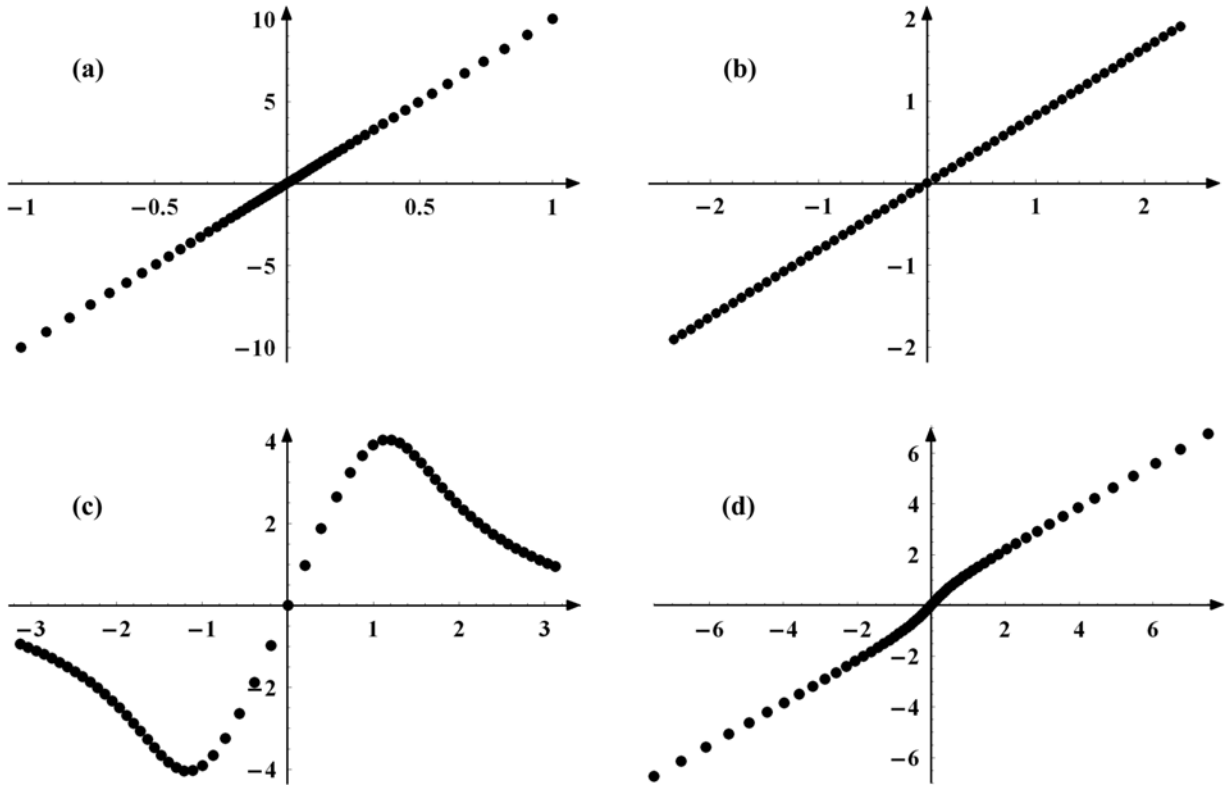

Figure 2. Sampling of the contour warp $-3 \leq y \leq 3$ with step 0.1: (a) (35), (b) (36), (c) (37) with $p = q = 0.1$, and (d) (38).

This system presents $2\frac{A}{h} + 1$ equations with $2\frac{A}{h} + 1$ unknowns, i.e., $F_+(hi)$ with $i = 0, \pm 1, \pm 2, .. \pm\frac{A}{h}$. The solution of this system leads to the following representation of the W-H unknowns:

$$F_+(\alpha) \approx F_{+a}(\alpha) = G^{-1}(\alpha) \cdot \left[-\frac{h}{2\pi j} \sum_{i=-A/h}^{A/h} m(\alpha, hi) F_+(hi) + \frac{R}{\alpha - \alpha_o} \right] \tag{33}$$

$$F_-(\alpha) \approx F_{-a}(\alpha) = -\frac{h}{2\pi j} \sum_{i=-A/h}^{A/h} m(\alpha, hi) F_+(hi) + \frac{R}{\alpha - \alpha_o} \tag{34}$$

The accuracy of the numerical solution depends on the parameters A and h. To improve the accuracy the discretization step h has to be chosen as small as possible and the parameter A has to be chosen as large as possible. Moreover, the choice of an elementary quadrature is relevant to demonstrate the high convergence rate of the proposed formulation.

4.1. Contour Warps to Improve the Numerical Convergence

[30] Generally the numerical solution of Fredholm integral equation of second kind is very efficient even using simple numerical quadrature. From theoretical considerations [*Kantorovich and Krylov*, 1958] we ascertain that by diminishing h and increasing A the numerical solution converges to the exact solution of the integral equation. However, we experience slow convergence and degradation of numerical precision when we deal with equations where the singularities of source and/or kernel are critical, i.e., near the integration path. This problem are well known in literature, see for example [*Kantorovich and Krylov*, 1958]. There are several techniques to overcome this problem, for example we can apply specialized numerical quadrature. We suggest a different approach which is based on warping the contour path: in particular we warp the real α axis into a new contour, far enough from the critical singularities. This method has been already used with success by the authors to factorized matrices of order 4 in diffraction problems: diffraction by

a plane wave at skew incidence on an arbitrary impenetrable wedge immersed in an homogeneous material [see *Daniele and Lombardi*, 2006]. Let us define $\lambda(y)$ as a line on the α plane located enough far from the critical points of the Fredholm equation.

[31] For instance, in wedge problems [*Daniele and Lombardi*, 2006], the critical point includes the branch points $\pm k$ (where k is the propagation constant) and the pole α_o (source pole of the incident plane wave). In order to avoid critical points near the integration line for slightly lossy media, we introduce the special contour defined by *Daniele and Lombardi* [2006]:

$$\lambda(y) = -k\cos\left(-\frac{\pi}{2} + jy\right), \quad -\infty < y < \infty \tag{35}$$

This contour joins the points $\pm jk$ with a straight α line.

[32] We have tested several different kind of contour warps. The optimal choice of the contour $\lambda(y)$ is based on the study of the spectrum of the W-H problem, i.e., the source and the kernel. For example we suggest the use of (35) and (36) for spectrum with singularities in the second and fourth quadrant, and the use of (37) with singularities with small imaginary part near 0. Another useful contour warp is (38).

$$\lambda(y) = ke^{j\frac{\pi}{4}}y, \quad -\infty < y < \infty \tag{36}$$

$$\lambda(y) = k\left[y + j\frac{\arctan y}{p + qy^2}\right], \quad -\infty < y < \infty \tag{37}$$

where p and q are positive parameters,

$$\lambda(y) = -k\cos\left(-\frac{\pi}{2} + \frac{gd(y)}{2} - jy\right), \quad -\infty < y < \infty \tag{38}$$

where $gd(y) = \arccos(\frac{1}{\cosh(y)})sign(y)$ is the Gudermann's function. Figure 2 reports the contour warps (35)–(38).

[33] Note that if we sample y with uniform distribution, we can generate samples with non uniform distribution in the original domain α. This is a special feature that can influence the convergence of the quadrature.

[34] If no singularity of $G(\alpha)$ and $G^{-1}(\alpha)$ is present in the region between real α axis and $\lambda(y)$, the contour warp reduces the Fredholm equation (22) to the equation:

$$F_+(\alpha(y)) = -\frac{G^{-1}(\alpha(y))}{2\pi j} \cdot \int_{-\infty}^{+\infty} \frac{[G(t(x)) - G(\alpha(y))]F_+(t(x))}{t(x) - \alpha(y)} t'(x)dx + \frac{G^{-1}(\alpha(y))R}{\alpha(y) - \alpha_o} \tag{39}$$

where $-\infty < y < \infty$ and where $t(y) = \alpha(y) = \lambda(y)$ for a given $\lambda(y)$. The discretized version of (39) is:

$$G(\alpha(y)F_+(\alpha) + \frac{h}{2\pi j}\sum_{i=-A/h}^{A/h} m(\alpha(y), t(h\,i))F_+(t(h\,i))t'(hi) = \frac{R}{\alpha(y) - \alpha_o} \tag{40}$$

and it yields the following linear system of $2\frac{A}{h} + 1$ equations where the $2\frac{A}{h} + 1$ unknowns are $F_+(t(hi))$:

$$G(\alpha(h\,r)F_+(h\,r) + \frac{h}{2\pi j}\sum_{i=-A/h}^{A/h} m(\alpha(h\,r), t(h\,i))F_+(t(h\,i))t'(h\,i) = \frac{R}{\alpha(h\,r) - \alpha_o} \tag{41}$$

with $r = 0, \pm 1, \pm 2, .., \pm\frac{A}{h}$. The approximate solution for the W-H unknowns in the α plane is:

$$F_{+a}(\alpha) = G^{-1}(\alpha)\left[-\frac{h}{2\pi j}\sum_{i=-A/h}^{A/h} m(\alpha, t(h\,i))F_+(h\,i)t'(hi) + \frac{R}{\alpha - \alpha_0}\right] \tag{42}$$

$$F_{-a}(\alpha) = -\frac{h}{2\pi j}\sum_{i=-A/h}^{A/h} m(\alpha, t(h\,i))F_+(t(h\,i))t'(hi) + \frac{R}{\alpha - \alpha_0} \tag{43}$$

4.2. Analytical Continuation Outside the Integration Line

[35] Equations (42) and (43) provide the approximate representation of $F_+(\alpha)$ and $F_-(\alpha)$ in the whole α plane through the analytical continuation of the numerical solutions obtained on the integration line $\lambda(y)$. When branch lines are present the analytical continuation is a critical procedure: in fact, the analytical continuation provides correct results only for the principal branch of $F_+(\alpha)$ and $F_-(\alpha)$. For instance in wedge diffraction problems it is convenient to define the Sommerfeld functions to represent the diffracted field (these functions are defined in the w plane where $\alpha = -k\cos(w)$) [*Daniele and Lombardi*, 2006]. The relation between the Sommerfeld functions and the W-H solutions needs the introduction of other branch of $F_+(\alpha)$ besides the

principal one. The extension of the solution $F_{+a}(\alpha)$ on other branches is described by *Daniele and Lombardi* [2006] and it uses difference equations derived from the W-H equations.

[36] Moreover we observe the following important aspects: (1) the approximate solutions (42) and (43) introduce spurious poles and (2) in specific problems it is important to evaluate residues of $F_+(\alpha)$ and $F_-(\alpha)$ in points that are structural singularities (zeroes of det[G(α)] and/or det[$G^{-1}(\alpha)$]). For what concerns aspect 1, we observe that the exact representation of $F_+(\alpha)$, see (44), shows a compensation of the minus structural singularities (poles or branch points located in the upper half plane $Im[\alpha] > 0$) in the second member.

$$F_+(\alpha) = -\frac{1}{2\pi j}\int_{-\infty}^{+\infty}\frac{G^{-1}(\alpha)[G(\alpha)-G(t)]F_+(t)}{\alpha - t}dt + G^{-1}(\alpha)\frac{R}{\alpha-\alpha_o}, \quad Im[\alpha_o] < 0 \tag{44}$$

In fact if we suppose the presence of the zero α_c of det[G(α)] in $Im[\alpha] > 0$, we obtain that the residue of the integral part in (44) is:

$$R_{\alpha_c} = -\frac{1}{2\pi j}\mathrm{Res}\left[G^{-1}(\alpha)\right]_{\alpha_c}\int_{-\infty}^{+\infty}\frac{-G(t)F_+(t)}{\alpha_c - t}dt = \frac{1}{2\pi j}\mathrm{Res}\left[G^{-1}(\alpha)\right]_{\alpha_c}\int_{-\infty}^{+\infty}\frac{F_-(t)}{\alpha_c - t}dt \tag{45}$$

Taking into account that $F_-(\alpha)$ presents only the pole α_o with residue R in the half plane $Im[\alpha] < 0$, we obtain:

$$R_{\alpha_c} = \frac{1}{2\pi j}\mathrm{Res}\left[G^{-1}(\alpha)\right]_{\alpha_c}\int_{-\infty}^{+\infty}\frac{F_-(t)}{\alpha_c - t}dt = -\mathrm{Res}\left[G^{-1}(\alpha)\right]_{\alpha_c}\frac{R}{\alpha_c-\alpha_o} \tag{46}$$

Since the second term of (44) (nonintegral part) presents a residue in α_c that compensates the one in the integral term of (44) (see (46)), the analytical exact representation of $F_+(\alpha)$ does not present spurious poles located in the upper half plane ($Im[\alpha] > 0$). Consequently we state that $F_+(\alpha)$ is a standard plus function.

[37] Similar considerations can be done if the kernel (or its inverse) presents a branch line in the upper half plane ($Im[\alpha] > 0$). Let us suppose that a branch point α_c of $G^{-1}(\alpha)$ is located in $Im[\alpha] > 0$. We observe a compensation between the first and the second term in (44). The jump of the first term (integral term) along the two lips of the branch line is:

$$\begin{aligned}\Delta\left[\frac{1}{2\pi j}\int_{-\infty}^{+\infty}\frac{G^{-1}(\alpha)G(t)F_+(t)}{\alpha - t}dt\right] &= \Delta\left[G^{-1}(\alpha)\right]\frac{1}{2\pi j}\int_{-\infty}^{+\infty}\frac{F_-(t)}{\alpha - t}dt \\ &= -\Delta\left[G^{-1}(\alpha)\right]\frac{R}{\alpha-\alpha_o}\end{aligned} \tag{47}$$

where Δ represents the jump between the two lips. (47) is equal and opposite in sign to the jump of the second term

$$\Delta\left[G^{-1}(\alpha)\right]\frac{R}{\alpha-\alpha_o} \tag{48}$$

[38] Thus we conclude that in the exact analytical representation (44) we obtain a compensation effects for offending minus singularities, either poles or branch points.

[39] The compensation effect for offending singularities α_c ($Im[\alpha_c] > 0$) derives from the equality

$$\frac{1}{2\pi j}\int_{-\infty}^{+\infty}\frac{G(t)F_+(t)}{\alpha_c - t}dt = -\frac{R}{\alpha_c-\alpha_o} \tag{49}$$

that holds if α_c is located in the upper half plane $Im[\alpha] > 0$.

[40] If we evaluate numerically (44), we experience spurious singularities in the numerical solution $F_{+a}(\alpha)$ because of the presence of offending singularities in the kernel or its inverse. In fact the compensation effects does not hold exactly in the numerical representation.

[41] For example, when $G^{-1}(\alpha)$ contains an "offending" singularity α_c (located in $Im[\alpha] > 0$), the numerically sampled form of (49) is:

$$\frac{h}{2\pi j}\sum_{i=-A/h}^{i=A/h}\frac{G(hi)F_+(hi)}{\alpha_c - hi} \approx -\frac{R}{\alpha_c-\alpha_o} \tag{50}$$

The presence of a finite sum, instead of an exact integral along the real axis, does not guarantee the compensation effect of the analytical expression in (44). Therefore we may experience degradation of precision for the $F_{+a}(\alpha)$ when α is close to α_c and besides $F_{+a}(\alpha)$ may contains spurious singularities in its spectrum.

[42] The ascertain of the equality (50) in the upper half plane ($Im[\alpha] > 0$) is an accuracy index for the numerical solution $F_{+a}(\alpha)$, in particular for what concerns spurious

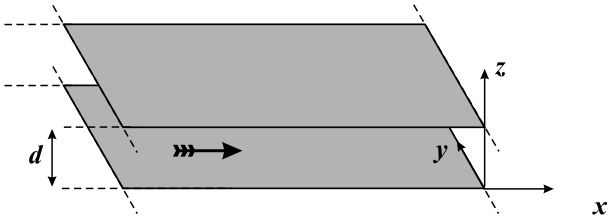

Figure 3. Example 1: the truncated planar waveguide.

offending singularities. Similar considerations hold for $F_{-a}(\alpha)$.

[43] For what concerns aspect 2, the evaluation of residues of $F_+(\alpha)$ in α_i points ($Im[\alpha_i] < 0$), that are structural singularities (zeroes of det[G(α)] and/or det[$G^{-1}(\alpha)$]), is usually very important in practical applications. For example, in the framework of waveguide scattering, the residues of $F_+(\alpha)$ are the excitation coefficients of modes with propagation constant α_i in closed structure located in the plus region. The evaluation of residue for structural singularities is often numerically unstable if we use approximate representations of $F_+(\alpha)$ as (42). To overcome this problem we observe that:

$$\mathrm{Res}[F_+(\alpha)]_{\alpha_i} = \mathrm{Res}\left[G^{-1}(\alpha)\right]_{\alpha_i} F_-(\alpha_i) \qquad (51)$$

where $G^{-1}(\alpha)$ is evaluated analytically, $F_-(\alpha)$ is regular in α_i and it can be numerically evaluated.

5. Numerical Validation

[44] In the following we compare exact factorizations with approximate factorizations obtained from the numerical solution of Fredholm integral equations as described in the previous sections. We recall that the spectrum of W-H kernels is related to the nature of structural singularities (branch point and/or poles). In the following we consider scattering/diffraction problems with scalar and matrix kernel whose spectrum is continuous, discrete or mixed.

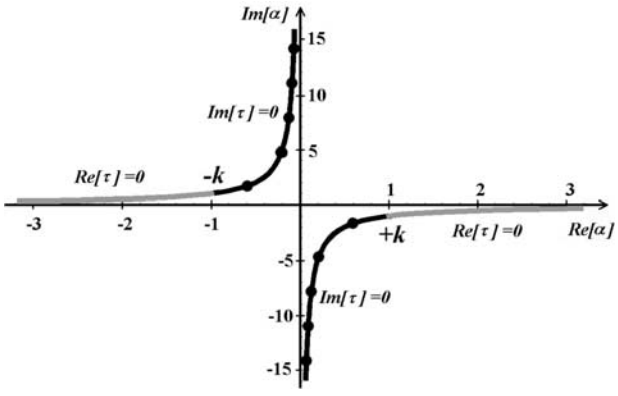

Figure 4. Example 1: spectrum of (54) with $\lambda = 1$, $k = \frac{2\pi}{\lambda}(1 - j)$, and $d = \lambda$.

5.1. Scalar Kernels

[45] Example 1 is an approximate factorization of a scalar kernel with a mixed spectrum. The following scalar kernel arises from the diffraction (or radiation) problem of a truncated planar waveguide of thickness d immersed in a free space medium with propagation constant k (see Figure 3):

$$g(\alpha) = \frac{\omega\varepsilon}{\sqrt{k^2 - \alpha^2}} \frac{e^{j\sqrt{k^2-\alpha^2}\,d}}{\cos\left[\sqrt{k^2 - \alpha^2}d\right]} \qquad (52)$$

where ω is the angular frequency and ε the permittivity of the medium. Since $g(\alpha)$ yields an integral equation with non compact operator $m(\alpha, t)$ (31) and since the factorization of $\frac{1}{\sqrt{k^2-\alpha^2}}$ is known in closed form

$$\frac{1}{\sqrt{k^2 - \alpha^2}} = \frac{1}{\sqrt{k - \alpha}} \frac{1}{\sqrt{k + \alpha}} \qquad (53)$$

let us consider the factorization problem of the following normalized kernel $G(\alpha)$

$$G(\alpha) = \frac{e^{j\sqrt{k^2-\alpha^2}\,d}}{\cos\left[\sqrt{k^2 - \alpha^2}d\right]} = G_-(\alpha)G_+(\alpha) \qquad (54)$$

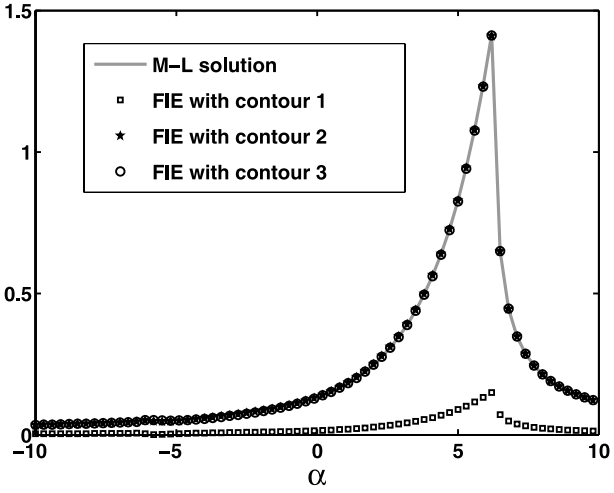

Figure 5. Example 1: $|F_+(\alpha)|$ obtained using the approximate analytical approach (reference solution M-L) and the approximate numerical Fredholm approach (FIE) with the proposed different contours 1, 2, and 3.

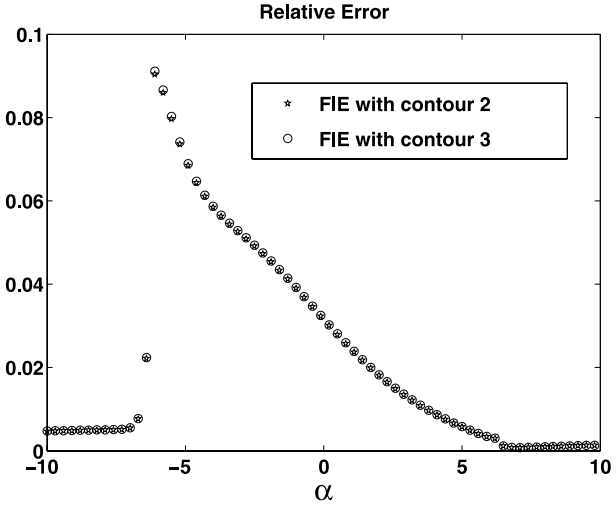

Figure 6. Example 1: relative error along the real axis α obtained using contour 2 and contour 3.

From $G(\alpha)$ we obtain a Fredholm integral equation of second kind, since the Fredholm kernel $m(\alpha, t)$ (31) is a compact operator. Note that:

$$g_+(\alpha) = \frac{\sqrt{\omega\varepsilon}}{\sqrt{k-\alpha}}\, G_+(\alpha) \tag{55}$$

[46] Using the Mittag-Leffler (M-L) expansion the factorized functions $G_+(\alpha)$ and $G_-(\alpha)$ are known and are given by the following expressions [*Daniele*, 2004]:

$$G_+(\alpha) = \frac{\Gamma\left(-\frac{\alpha}{A_d}+\frac{B}{A_d}+1\right)\exp\left[\frac{\tau d}{\pi}\log\frac{j\tau-\alpha}{k} - q\,\alpha\right]}{\sqrt{\cos(kd)}\, e^{\gamma\frac{\alpha}{A_d}}\Gamma\left(\frac{B}{A_d}+1\right)} \cdot \prod_{n=1}^{\infty}\frac{\left(1-\frac{\alpha}{A_d n+B}\right)}{\left(1-\frac{\alpha}{\alpha_n}\right)} \tag{56}$$

$$G_-(\alpha) = G_+(-\alpha) \tag{57}$$

where $\tau = \sqrt{k^2-\alpha^2}$, $A_d = -j\frac{\pi}{d}$, $B = -\frac{1}{2}A_d$, $q = j\frac{d}{\pi}[\log(-\frac{j2\pi}{kd}) + 1 - \gamma]$ and where $\Gamma(\alpha)$ and γ are respectively the Euler gamma function and the Euler-Mascheroni constant. The spectrum of $G(\alpha)$ is a mixed spectrum for the presence of simple poles $\alpha = \pm\alpha_n$, $n \in \mathbf{N_0}$ besides the branch points $\pm k$. The poles α_n are:

$$\alpha_n = \sqrt{k^2 - \left(\frac{(n-1/2)\pi}{d}\right)^2}, \quad n \in \mathbf{N_0}, \quad Im[\alpha_n] < 0 \tag{58}$$

Without loss of generality, in order to highlight the properties of kernel, Figure 4 shows the spectrum of $G(\alpha)$ for $\lambda = 1$ (wavelength), $k = \frac{2\pi}{\lambda}(1-j)$, $d = \lambda$. Figure 4 reports the poles $\pm\alpha_n$ as dots, while the

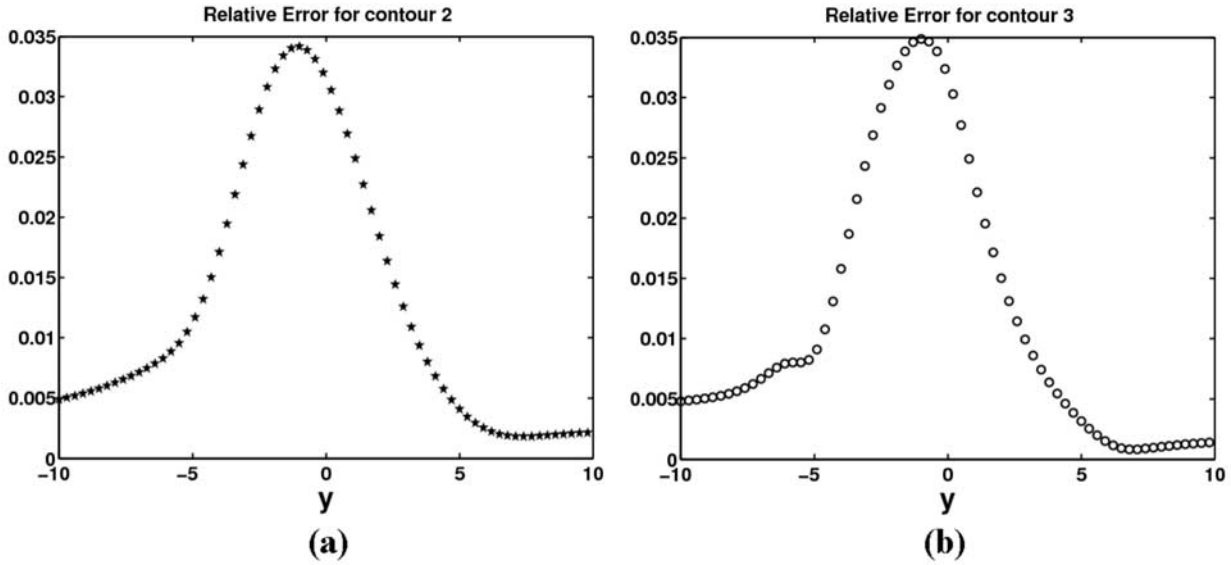

Figure 7. Example 1: Relative error along the contours 2 and 3 (y is the parameter of the two contours).

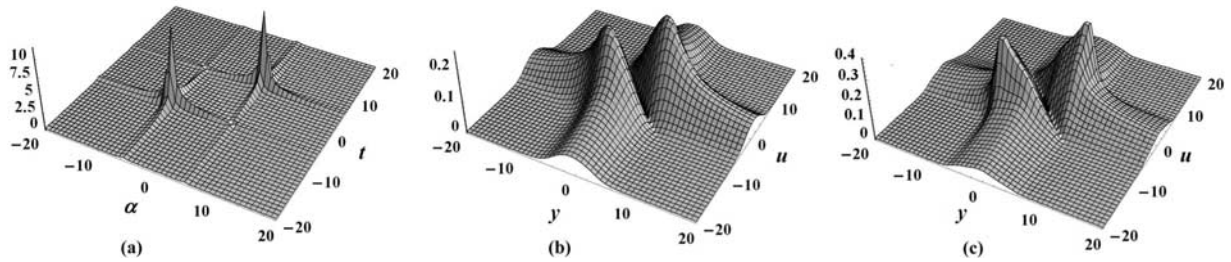

Figure 8. Example 1: Spectral properties of kernel $m(\alpha, t)$ along the three different contours. (b) and (c) Plotted versus the parameter of the contours, i.e., plots of $m(\lambda(y), \lambda(u))$.

continuous lines are referred to branch lines. In practical cases (small imaginary part of k) we have arcs of hyperbola and poles very close to the real axis. The use of warp, as described in section 4.1, is useful to improve the numerical convergence of line integral in the Fredholm integral equation when singularities are close to the real axis.

[47] In the following we compare numerical results obtained using three different contours to solve the Fredholm integral equation. The reference approximate solution is obtained from (56)–(57) truncating the infinite product to a given number N of terms. The three contours are: 1) the real axis, 2) $\lambda(y) = Re[k]\, e^{j\frac{\pi}{4}}\, y$ and 3) $\lambda(y) = Re[k](y + j \arctan(y))$ with $-\infty < y < +\infty$. To investigate the convergence we have chosen the following parameters:(1) the physical parameters $\lambda = 1$, $k = \frac{2\pi}{\lambda}(1 - j10^{-8})$, and $d = 1.1\frac{\lambda}{2}$, (2) the source the fundamental mode of the planar waveguide $\alpha_s = \alpha_1$ with excitation coefficient equal to 1 ($\alpha_1 = 5.597 - \jmath 7.054 \times 10^{-8}$), (3) the quadrature parameters $A = 40$ and $h = 0.2$, and (4) the truncation of products $N = 200$.

[48] Figure 5 shows the plots of $|F_+(\alpha)|$ obtained using the approximate analytical approach (reference solution M-L) and the Fredholm approach, see (41)–(43), with the proposed different contours. Note that the reference solution and the numerical solution obtained with contours 2 and 3 are indistinguishable, on the contrary using contour 1 (the real axis α) we obtain uncorrect results. This substantial degradation of the solution is due to the presence of singularities very close to the integration path: the branch points $\pm k$ and the poles $\pm\alpha_n$ are with very small imaginary part.

[49] Figures 6 and 7 show the relative error obtained using contour 2 and contour 3 with respect to the reference solution respectively along the real axis α (Figure 6) and versus the parameter of the contour y (Figure 7).

[50] In order to understand the effect of the contour warp on the Fredholm integral equation, let us consider its kernel $m(\alpha, t)$ (31) along the three different contours. The spectral properties are summarized in Figure 8. Note that the spectrum is more concentrated and smooth along the contours 2 and 3.

[51] In order to investigate the accuracy in depth we evaluate the residue of $F_-(\alpha)$ in the pole $-\alpha_1$. If we use the full kernel $g(\alpha)$ instead of $G(\alpha)$, this residue is the reflection coefficient of the fundamental mode due to the truncation of the planar waveguide.

[52] Note that the evaluation of this residue is often unstable if we use approximate representation of $F_-(\alpha)$, see section 4.2. To overcome this problem we use the following property obtained from the W-H equation (1):

$$\mathrm{Res}[F_-(\alpha)]|_{-\alpha_1} = \mathrm{Res}[G(\alpha)]|_{-\alpha_1} F_+(-\alpha_1) \qquad (59)$$

where $F_+(-\alpha_1)$ is analytical in $-\alpha_1$ and $G(\alpha)$ is known in closed form. $F_+(-\alpha_1)$ determines the precision of residue $\mathrm{Res}[F-(\alpha)]|_{-\alpha 1}$. See Table 1 to compare the values of $F_+(-\alpha_1)$ obtained from the approximate solution with the three suggested contours with respect to the one obtained from the reference solution. Note that contour 1 yields error on the evaluation of $F_+(-\alpha_1)$ as expected from Figure 5.

[53] The accuracy of the numerical solution depends on the parameters A and h, besides the choice of the contour warp. To improve the accuracy the discretization step h has to be chosen as small as possible and the parameter A (truncation of the integration interval) has to be chosen as large as possible. Besides the choice of an elementary quadrature is relevant to demonstrate the convergence of the proposed formulation. Specialized quadrature can improve the convergence.

5.2. Rational Matrix Kernels

[54] The Wiener-Hopf formulation of practical problems usually involves matrix kernels. The central problem in solving vector Wiener-Hopf equations is the factorization of a $n \times n$ matrix. An important family of

Table 1. Example 1: Estimation of $F_+(-\alpha_1)$

	Ref.	Contour 1	Contour 2	Contour 3
$Re[F_+(-\alpha_1)]$	−0.0482257	−0.000549844	−0.0455368	−0.0483479
$Im[F_+(-\alpha_1)]$	+0.0117099	+0.000242659	+0.0147477	+0.0157931

matrix kernels are the ones whose elements are rational functions, i.e., rational matrix kernels. Since the exact factorization of such kernels is available in literature [*Bart et al.*, 1979], in this section we validate the Fredholm factorization for this class of matrices. Besides, to overcome cumbersome factorization techniques, we present a new simple procedure to factorize rational matrix kernels (see Appendix A). This procedure is applied to find exact factorized matrices in Example 2 and 3.

5.2.1. Example 2: Rational Matrices of Order 2

[55] In this example we consider the Wiener-Hopf problem

$$G(\alpha)F_+(\alpha) = F_-(\alpha) + \frac{R}{\alpha - \alpha_o} \tag{60}$$

whose kernel is a rational matrix of order 2 of the following kind:

$$G(\alpha) = \begin{pmatrix} 1 & jq\dfrac{a^2+\alpha^2}{b^2+\alpha^2} \\ jq & 1 \end{pmatrix} = G_-(\alpha)G_+(\alpha) \tag{61}$$

With this example we want to show all the capabilities of the Fredholm factorization; thus we present the following tests: (1) factorization of kernel using the procedure of section 2 together with the Fredholm method (sections 3–4) for a given fictitious pole α_p, (2) solution of the W-H problem (60) for given sources $\alpha_o \neq \alpha_p$ using the factorization found in test 1; and (3) the factorized matrices (obtained using different methods) differs from each other up to a premultiplicative constant matrix: evaluation of the constant matrix.

[56] The exact factorization is obtained for example simply using the analytical method proposed in Appendix A:

[57] The numerical tests 1–3 are performed with the following parameters: $a = 1$, $b = 2$, and $q = 0.5$.

[58] In tests 1–2, the Fredholm approximate solutions are obtained with the method discussed in this paper. In order to use the Fredholm approximate method it is important to ascertain the location of the structural singularities, i.e., the zeroes of $\det[\mathrm{G}(\alpha)]$ and $\det[\mathrm{G}^{-1}(\alpha)]$. The structural poles are: $\pm j1.84391$ and $\pm j2$. These poles are rather far from the real axis; therefore no contour warp is applied in the Fredholm approximate method. By assuming a fictitious source pole $\alpha_p = 1 - j0.1$, the integration parameters $A = 10$ and $h = 0.1$ we apply the Fredholm procedure to (12). Using (7)–(8) we numerically obtain the factorized matrices $G_-(\alpha)$, $G_+(\alpha)$.

[59] In order to validate the Fredholm procedure, we compare the solution $F_+(\alpha)$ obtained using the Fredholm approximated factorization with respect to the exact solution obtained from (62) and (63).

[60] We recall that:

$$F_+(\alpha) = G_+^{-1}(\alpha)G_-^{-1}(\alpha_o)\frac{R}{\alpha - \alpha_o} \tag{64}$$

[61] The source pole is $\alpha_o \neq \alpha_p$ and the source coefficient R is a combination of the canonical basis:

$$R = R_1 + 0.5R_2 \tag{65}$$

where $R_1 = \begin{vmatrix} 1 \\ 0 \end{vmatrix}$, $R_2 = \begin{vmatrix} 0 \\ 1 \end{vmatrix}$.

[62] We have selected three values of α_o which are quite different from α_p: $\alpha_o = \pm j0.1$ and $\alpha_o = 1 + j$. The two source poles $\alpha_o = \pm j0.1$ give $F_+(\alpha)$ that differ from each other almost only in the phase.

$$G_-(\alpha) = \begin{vmatrix} \dfrac{j\left(\sqrt{b^2+a^2q^2} + j\sqrt{1+q^2}\alpha\right)}{\left(-b\sqrt{1+q^2} + \sqrt{b^2+a^2q^2}\right)(b+j\alpha)} & \dfrac{1}{bq - \frac{q\sqrt{b^2+a^2q^2}}{\sqrt{1+q^2}}} \\ 0 & -\dfrac{j}{-b + \frac{\sqrt{b^2+a^2q^2}}{\sqrt{1+q^2}}} \end{vmatrix} \tag{62}$$

$$G_+(\alpha) = \begin{vmatrix} 0 & \dfrac{\left(-b\sqrt{1+q^2} + \sqrt{b^2+a^2q^2}\right)\left(\sqrt{b^2+a^2q^2} - j\sqrt{1+q^2}\alpha\right)}{q(b-j\alpha)} \\ bq - \dfrac{q\sqrt{b^2+a^2q^2}}{\sqrt{1+q^2}} & -\dfrac{\left(bq - \frac{q\sqrt{b^2+a^2q^2}}{\sqrt{1+q^2}}\right)(jb+\alpha)}{q(b-j\alpha)} \end{vmatrix} \tag{63}$$

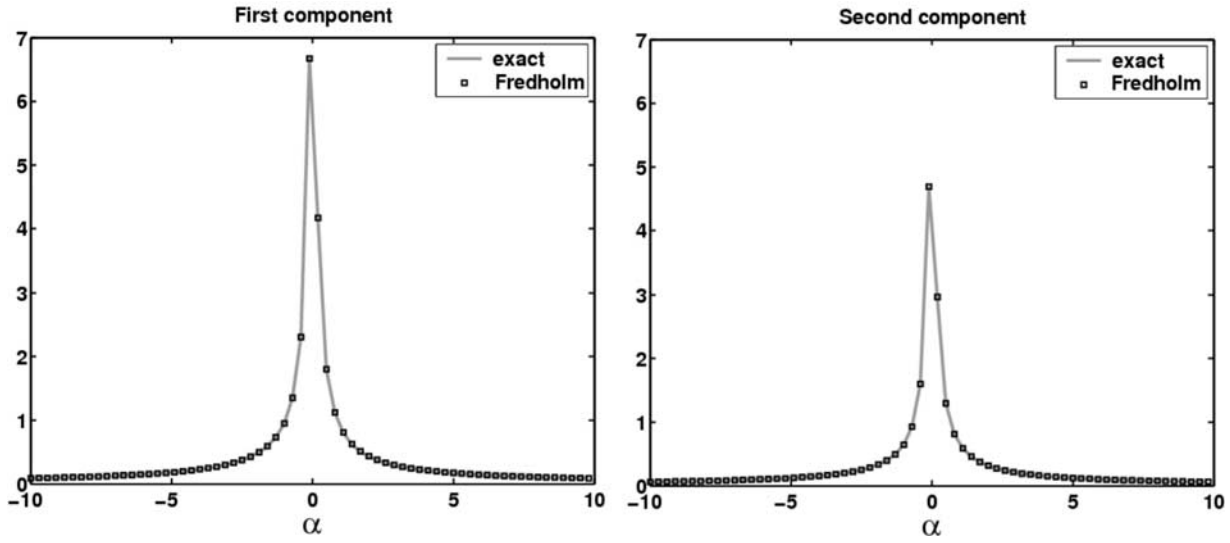

Figure 9. Example 2: $|F_+(\alpha)|$ components obtained using the analytical approach (reference solution) and the approximate numerical Fredholm approach for $\alpha_o = \pm j0.1$ (the two cases overlap in absolute value).

[63] Figure 9 reports the absolute value of the $F_+(\alpha)$ components obtained using the exact factorization and the Fredholm factorization with $\alpha_o = \pm j0.1$.

[64] Figure 10 reports the relative error per $F_+(\alpha)$ component. Note that the importance of the relative error has to be correlated with the intensity of the solution. We observe that the relative errors for $\alpha_o = \pm j0.1$ are very similar.

[65] Figures 11a and 11b report the absolute value of the $F_+(\alpha)$ components obtained using the exact factorization and the Fredholm factorization for $\alpha_o = 1 + j$. Besides Figures 11c and 11d report the relative error per $F_+(\alpha)$ component. Note that the analytical continuation of the approximate Fredholm solution shows a wide range of validity.

[66] In test 3, we recall that the factorized matrix $G_+(\alpha)$ can be defined up to a multiplicative constant matrix. The change of the arbitrary point α_p on the evaluation of $G_+(\alpha)$ yields different $G_+(\alpha, \alpha_p)$ matrices, see (14) and (15). For example if we compare the $G_{+,-}(\alpha)$

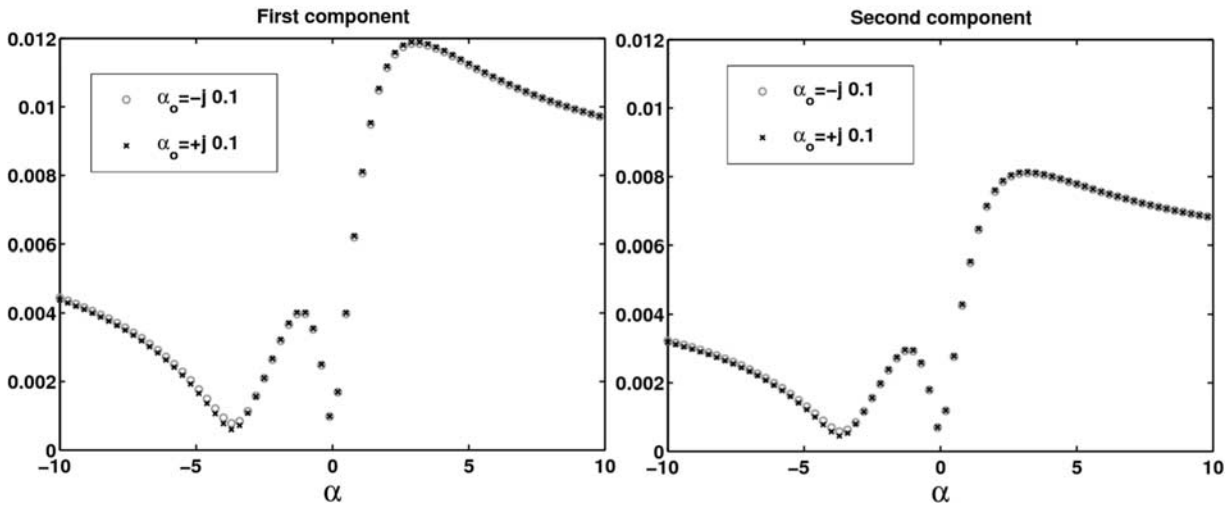

Figure 10. Example 2: relative errors of the $|F_+(\alpha)|$ components obtained using the Fredholm approach with respect to the analytical solution for $\alpha_o = \pm j0.1$.

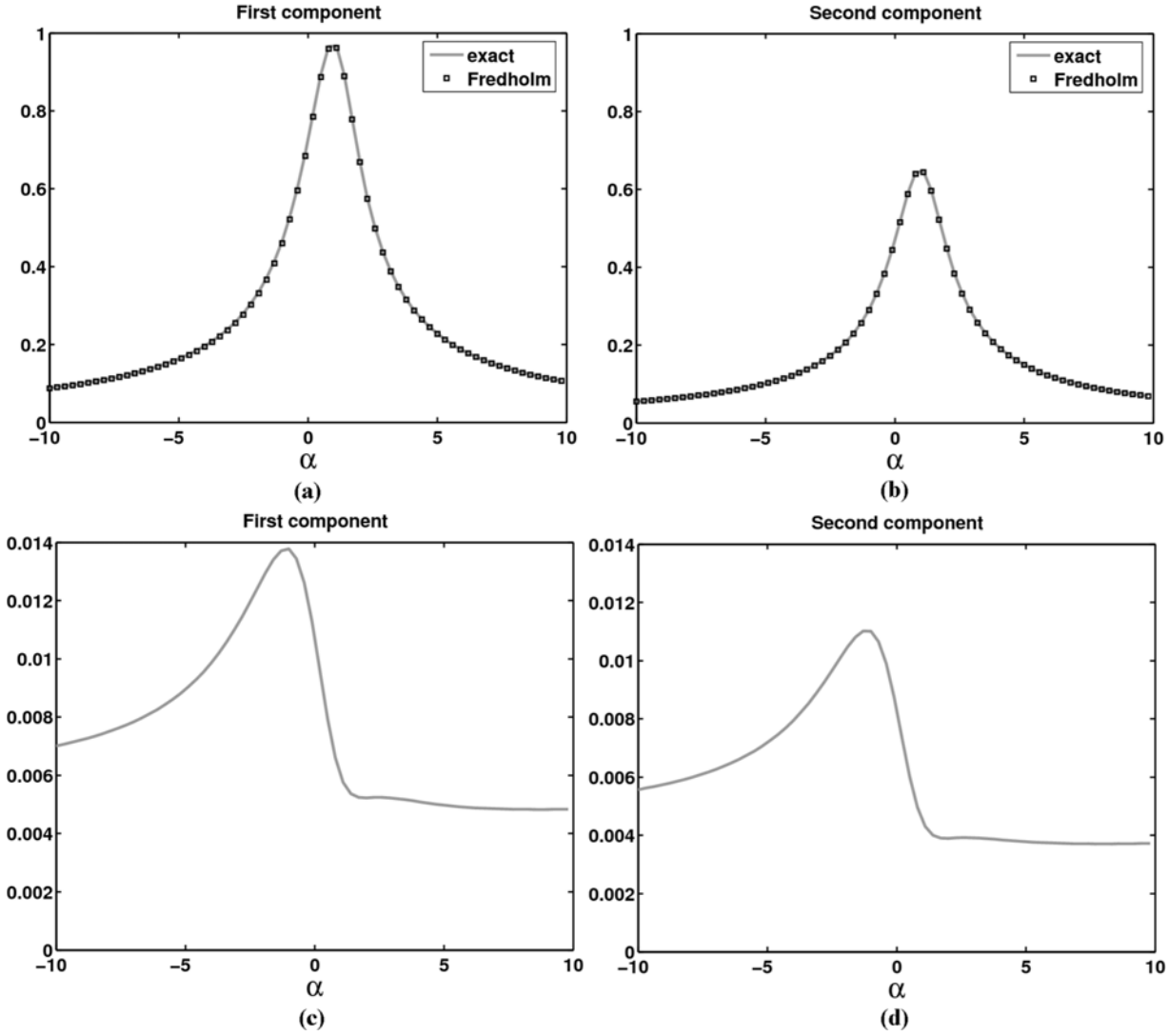

Figure 11. Example 2: (a)–(b) $|F_+(\alpha)|$ components obtained using the analytical approach (reference solution) and the Fredholm approach for $\alpha_o = 1 + j$ and (c)–(d) relative errors.

obtained from the analytical expressions (62)–(63) and the ones obtained using the Fredholm approach ($G^{(F)}_{+,-}(\alpha)$) with $\alpha_p = 1 - j0.1$ we obtain different expressions which differs up to the following premultiplicative constant matrix

$$K = \begin{vmatrix} 0.154055 - j6.01646 & 12.8130 \\ 0 & 6.40651 \end{vmatrix} \tag{66}$$

that is,

$$\begin{cases} KG_+(\alpha) = G^{(F)}_+(\alpha) \\ G_-(\alpha) = G^{(F)}_-(\alpha)K \end{cases} \tag{67}$$

in particular:

$$KG_+(\alpha) = \begin{vmatrix} 1 & \frac{-0.329107 - j0.11085 - (0.0601167 - j0.347788)\alpha}{2j+\alpha} \\ j0.5 & 1 \end{vmatrix} \tag{68}$$

[67] The evaluation of K can be obtained by sampling and comparing $G_{+,-}(\alpha)$ and $G^{(F)}_{+,-}(\alpha)$ in one point: a characteristic point is the origin of the α plane ($0 + j0$).

[68] Figure 12 shows one of the most significant components of the factorized kernel, $G_+(\alpha)_{12}$, and the

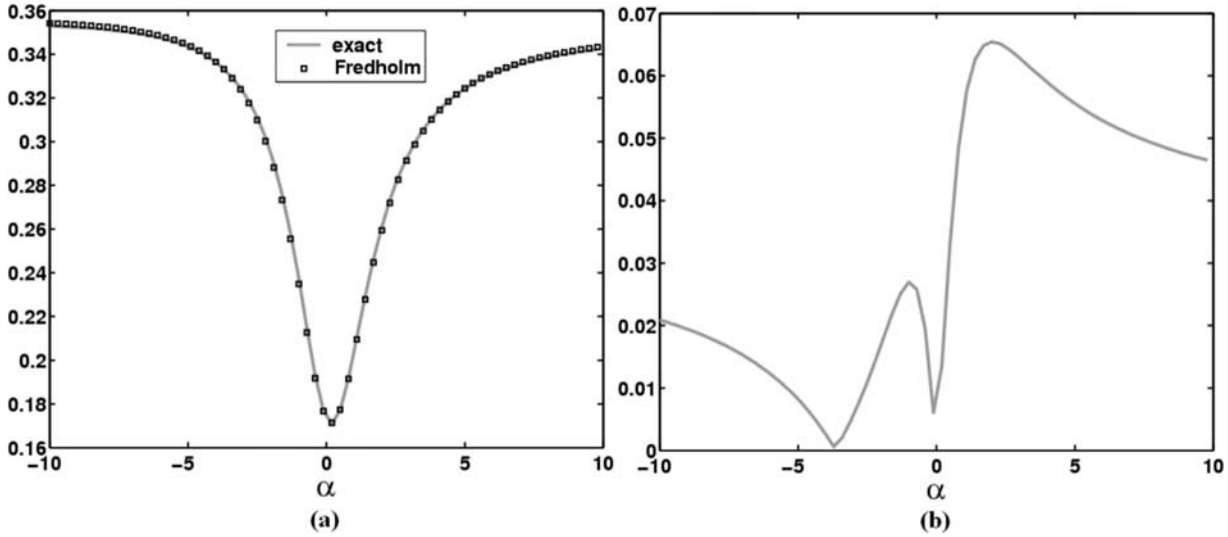

Figure 12. Example 2: (a) $|KG_+(\alpha)|_{12}$ component obtained using the analytical approach (reference solution) and $|G_+^{(F)}(\alpha)|_{12}$ obtained using the Fredholm approach and (b) relative error.

relative error obtained using the Fredholm approach with respect to the analytic approach.

5.2.2. Example 3: Rational Matrices of Order 3

[69] In this example we consider the Wiener-Hopf problem

$$G(\alpha)F_+(\alpha) = F_-(\alpha) + \frac{R}{\alpha - \alpha_o} \tag{69}$$

whose kernel is a rational matrix of order 3 of the following form:

$$G(\alpha) = \begin{pmatrix} \frac{j}{\alpha^2+1} & 2 & \frac{\alpha^2+4}{\alpha^2+1} \\ 1 & 2 & \frac{\alpha^2+9}{\alpha^2+1} \\ \frac{\alpha^2}{\alpha^2+1} & \frac{1}{\alpha^2+1} & 2 \end{pmatrix} \tag{70}$$

The source pole and the source coefficient in (69) are respectively $\alpha_o = -j2$ and $R = |1, 0, 0|^t$.

[70] We avoid to report the cumbersome exact factorized matrices that are obtained (for example) simply using the method proposed in Appendix A. The exact analytical solution is obtained using the exact factorized matrices and equation (3)–(4).

[71] In order to use the Fredholm approximate method it is important to ascertain the location of the structural singularities, i.e., the zeroes of det[G(α)] and det[$G^{-1}(\alpha)$]. The structural poles are reported in Figure 13: two of them are very close to the real axis thus we need to apply a contour warp to obtain good convergence in the numerical approach.

[72] By assuming the integration parameters $A = 20$ and $h = 0.1$, we compare the exact solution with the approximate Fredholm solution using different integration contours: 1) real axis 2) $\lambda(y) = ye^{-j\frac{\pi}{4}}$. Note that in the region between the real axis and the contour (2), no structural singularity is present.

[73] Figure 14 shows the absolute value of the factorized solution components $|F_+(\alpha)|$ obtained using the numerical approach with contour 1 and using the exact expressions; the relative error per $F_+(\alpha)$ component is reported, too. Figure 15 shows the absolute value of the factorized solution components $|F_+(\alpha)|$ obtained using the numerical approach with contour 2 and using the exact expressions; the relative error per $F_+(\alpha)$ component is reported, too. Note that Figure 15 is plotted along the parameter y of contour $\lambda(y)$. The importance of the relative error has to be correlated with the intensity of the solution.

5.3. Matrix Kernels With Mixed Spectrum

[74] Another important family of matrix kernels is the one whose elements contain terms that are irrational functions; that is, the kernel has continuous spectrum due to the presence of branch points in addition to the discrete spectrum due to the presence of poles. Closed form factorization of such kernels is not in general available; therefore the Fredholm approximate method can be one of the most powerful method to deal with this

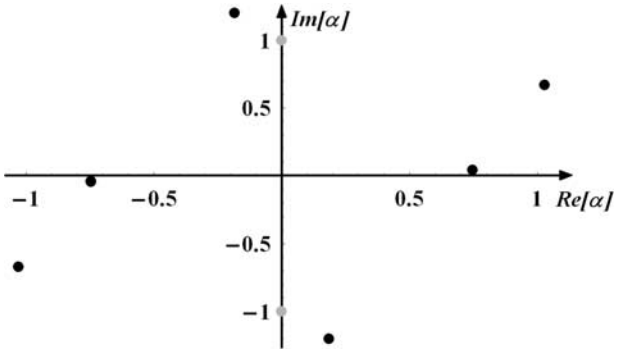

Figure 13. Example 3: spectrum of (70). Black dots are zeros of det[G(α)], and gray dots are zeros of det[$G^{-1}(\alpha)$].

kind of kernel. In this context, the authors of this paper have studied a practical engineering problem: diffraction by arbitrary impenetrable wedges (surface impedance) at skew incidence (see Figure 16). For further details on the 4×4 matrix kernel for wedge problems, see *Daniele and Lombardi* [2006]. In order to validate the Fredholm factorization, we consider the PEC (Perfect electric conductor) wedge at skew incidence (Example 4) where a closed form solution is available and well known in literature [see, e.g., *Daniele and Lombardi*, 2006]. In this problem the kernel is a matrix of order 4 and does not present poles; that is, its spectrum is continuous.

[75] With reference to Figure 16, we set the following physical parameters: wedge aperture angle $\Phi = 7\pi/8$, incident wave with zenithal angle $\beta = \pi/4$ and azimuthal angle $\varphi_o = 2\pi/3$, excitation $E_{zo} = 1$, $H_{zo} = 0$.

[76] Figure 17 shows the relative error of the GTD diffraction coefficient in $\log_{10}$ scale versus the azimuthal angle φ. The estimation of the GTD is obtained through the Fredholm approximate solution of the problem and the relative error is evaluated with respect to the exact solution.

[77] In particular, the top portion of Figure 17 reports the GTD diffraction coefficient (*dB*), while the bottom portion shows the relative error obtained from the Fredholm solution for different sets of quadrature param-

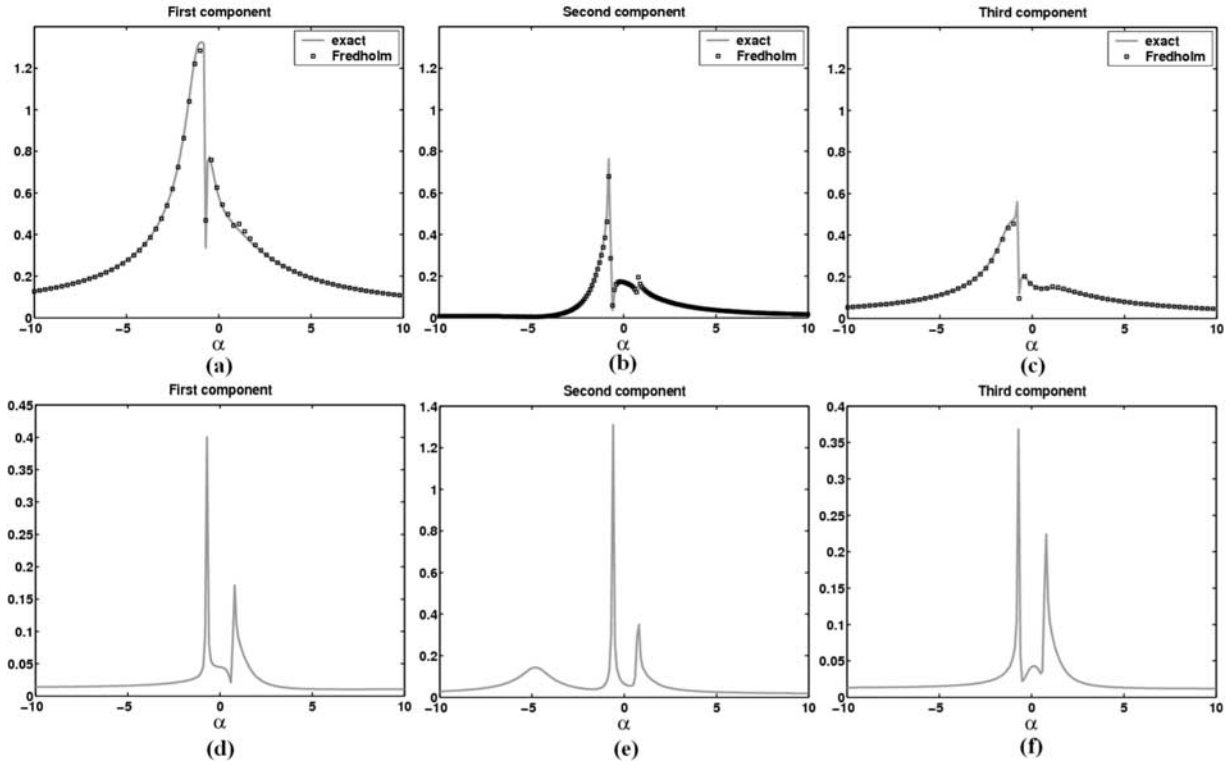

Figure 14. Example 3: (a)–(c) $|F_+(\alpha)|$ components obtained using the analytical approach (reference solution) and the Fredholm approach with contour 1 (real axis) and (d)–(f) relative error per $F_+(\alpha)$ component.

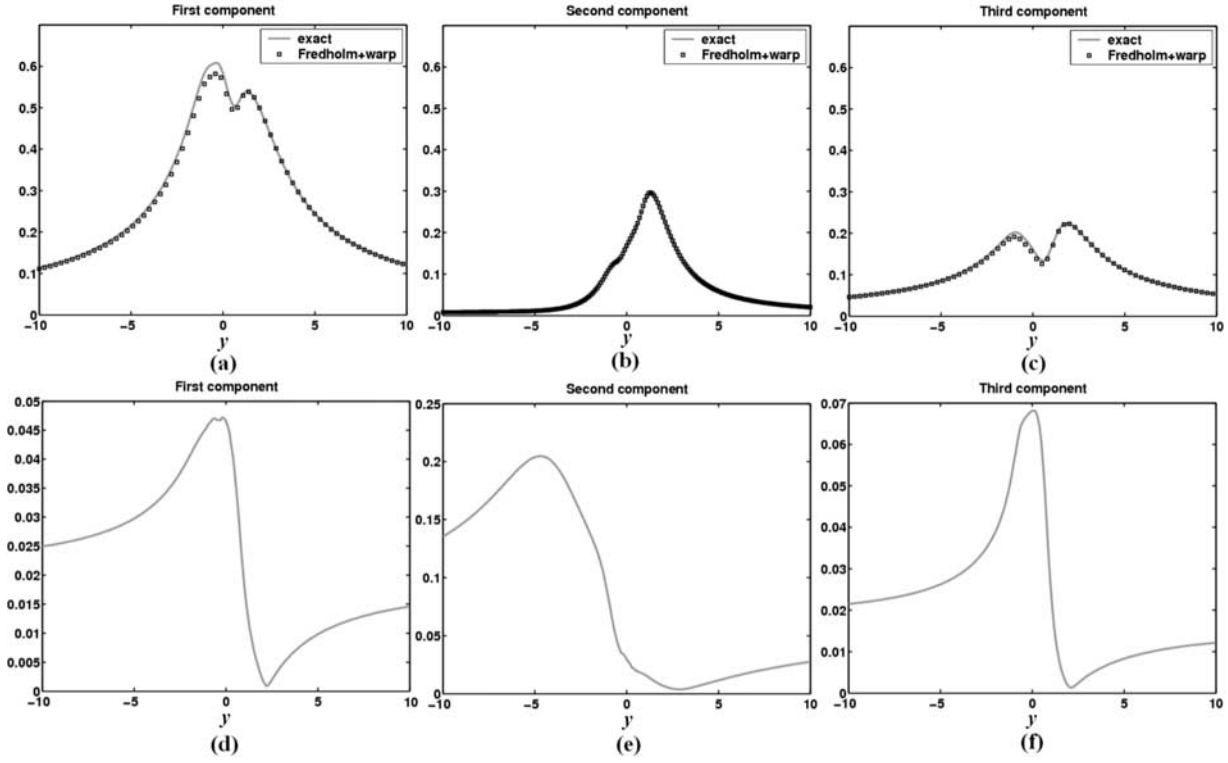

Figure 15. Example 3: (a)–(c) $|F_+(\alpha)|$ components obtained using the analytical approach (reference solution) and the Fredholm approach with contour 2 and (d)–(f) relative error per $F_+(\alpha)$ component. All plots are versus the parameter y of the contour 2.

eters (A, h) with respect to the exact value. Note that contour warp (35) is applied in the Fredholm solution. Figure 17 proves the convergence of the proposed method.

[78] We note that in the framework of wedge diffraction problems the use of Fredholm integral equations has been applied with success to the Sommerfeld-Malyuzhinets technique [see, e.g., *Budaev*, 1995; *Zhu and Lyalinov*, 2004; *Lyalinov and Zhu*, 2005].

[79] In the framework of Wiener-Hopf technique the use of Fredholm integral equations yields the general solution of impenetrable wedges with anisotropic impedance surfaces at skew incidence [*Daniele and Lombardi*, 2006]: diffraction components, surface waves and total field.

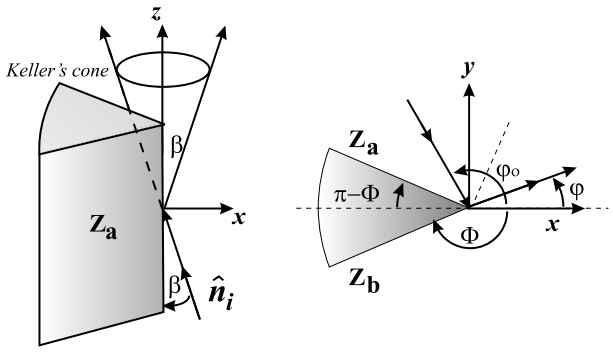

Figure 16. The impenetrable wedge at skew incidence.

6. Conclusion

[80] Mathematical and physical details relevant to a general theory of Wiener-Hopf factorization using Fredholm integral equation are presented.

[81] The Fredholm approach factorizes kernels of general form: matrix, scalar with arbitrary spectral properties. Several numerical tests validate this analytical-numerical technique to factorize W-H kernels of practical mathematical-physical and/or engineering problems. The paper shows the power and the versatility of the W-H formulation and the efficacy of reducing the W-H factorization

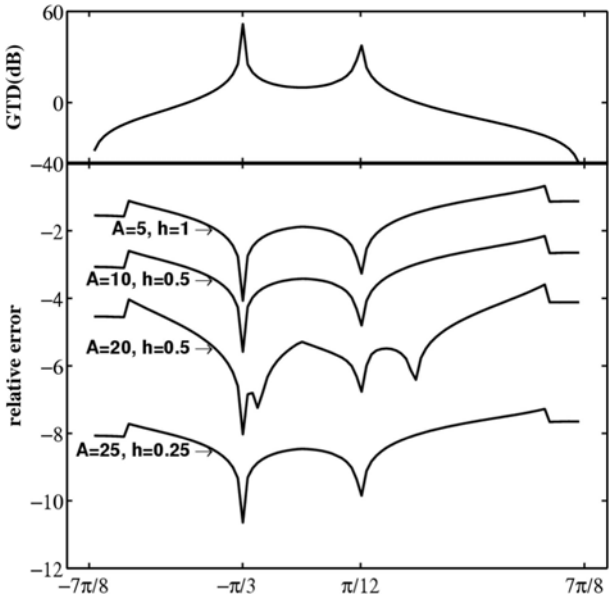

Figure 17. Example 4: GTD diffraction coefficient for PEC wedge and relative error of the Fredholm approximate estimate with respect to exact value.

problem to the approximate solution of Fredholm Integral equation of second kind.

Appendix A: New Procedure to Factorize Rational Kernel in Closed Form

[82] Let us consider a rational matrix $G(\alpha)$ and its inverse $G^{-1}(\alpha)$ of the following form:

$$G(\alpha) = \frac{A(\alpha)}{d(\alpha)}, \quad G^{-1}(\alpha) = \frac{B(\alpha)}{\delta(\alpha)} \tag{A1}$$

where $A(\alpha)$ and $B(\alpha)$ are polynomial matrices of order n, and $d(\alpha)$ and $\delta(\alpha)$ are scalar polynomials. In the following we suppose:

$$\frac{G(\alpha)}{\alpha} \to 0, \qquad \alpha \to \infty \tag{A2}$$

$$\frac{G^{-1}(\alpha)}{\alpha} \to 0, \quad \alpha \to \infty \tag{A3}$$

From section 2 the homogenous Wiener-Hopf equation (6) yields the factorized matrices (7). We recall equation (12) valid for $i = 1.n$:

$$G(\alpha)X_{i+}(\alpha) = \frac{U_{i-}(\alpha) - U_{i-}(\alpha_p)}{\alpha - \alpha_p} + \frac{U_{i-}(\alpha_p)}{\alpha - \alpha_p} \tag{A4}$$

By substituting (A1) we obtain:

$$\frac{A(\alpha)}{d(\alpha)}F_{i+}(\alpha) = F^s_{i-}(\alpha) + \frac{R_i}{\alpha - \alpha_p} \tag{A5}$$

where $R_i = U_{i-}(\alpha_p)$ is the canonical basis for the n-dimensional space and $F_{i+}(\alpha) = X_{i+}(\alpha)$ and $F^s_{i-}(\alpha) = \frac{U_{i-}(\alpha) - U_{i-}(\alpha_p)}{\alpha - \alpha_p}$ are respectively standard plus functions and standard minus functions, i.e., Laplace transforms. We define:

$$F_{i-}(\alpha) = F^s_{i-}(\alpha) + \frac{R_i}{\alpha - \alpha_p} \tag{A6}$$

Without lack of clarity in the following we suppress the subscript i in the equations and we denote the r zeroes of the denominator $d(\alpha)$ with $Im[\alpha] > 0$ and the s zeroes of the denominator $\delta(\alpha)$ with $Im[\alpha] < 0$ as follows

$$\{\alpha_\ell : d(\alpha_\ell) = 0 \quad Im[\alpha_\ell] > 0\} \tag{A7}$$

$$\{\gamma_\ell : \delta(\gamma_\ell) = 0 \quad Im[\gamma_\ell] < 0\} \tag{A8}$$

$\{\alpha_\ell\}$ and $\{\gamma_\ell\}$ are defined respectively the minus zeroes and the plus zeroes. Without loss of generality we consider the zeroes as simple zeroes. The zeroes $\{\alpha_\ell\}$ of $d(\alpha)$ induce poles in $F_-(\alpha)$:

$$F_-(\alpha) = \frac{R}{\alpha - \alpha_p} + \sum_{\ell=1}^{r} \frac{Q(\alpha_\ell)}{\alpha - \alpha_\ell} \tag{A9}$$

Similarly from:

$$F_+(\alpha) = \frac{B(\alpha)}{\delta(\alpha)}F_-(\alpha) \tag{A10}$$

we obtain:

$$F_+(\alpha) = G^{-1}(\alpha_p)\frac{R}{\alpha - \alpha_p} + \sum_{\ell=1}^{s} \frac{T(\gamma_\ell)}{\alpha - \gamma_\ell} \tag{A11}$$

The representations (A9) and (A11) introduce $r + s$ unknown vectors ($Q(\alpha_\ell)$ and $T(\gamma_\ell)$), i.e., $n(r + s)$ scalar unknowns. We enforce $n(r + s)$ equations using the equalities:

$$\frac{A(\alpha)}{d(\alpha)}F_+(\alpha) = F_-(\alpha) \quad \ell = 1.r \tag{A12}$$

$$F_+(\alpha) = \frac{B(\alpha)}{\delta(\alpha)}F_-(\alpha) \quad \ell = 1.s \tag{A13}$$

[83] From (A12) we obtain r vector equations (nr scalar equations):

$$\mathrm{Res}[F_-(\alpha)]_{\alpha=\alpha_\ell} = Q(\alpha_\ell) = \frac{A(\alpha_\ell)}{d'(\alpha_\ell)}F_+(\alpha_\ell), \quad \ell = 1.r \tag{A14}$$

From (A13) we obtain s vector equations (ns scalar equations):

$$\mathrm{Res}[F_+(\alpha)]_{\alpha=\gamma_\ell} = T(\gamma_\ell) = \frac{B(\gamma_\ell)}{\delta'(\gamma_\ell)} F_+(\gamma_\ell), \quad \ell = 1.s \tag{A15}$$

From the $n(r + s)$ scalar equations (A14) and (A15) we determine the residues $\{Q(\alpha_\ell)\}$ and $\{T(\gamma_\ell)\}$. Therefore from (A9) to (A11), the definition of $F_{+,-}(\alpha)$ and (7) we obtain the factorized matrices. Note that a generalization can be obtained considering the multiplicity of the poles $\{\alpha_\ell\}$ and $\{\gamma_\ell\}$ higher than 1.

[84] **Acknowledgments.** This work was supported by NATO in the framework of the Science for Peace Programme under the grant CBP.MD.SFPP 982376.

References

Abrahams, I. D. (2000), The application of Pade approximants to Wiener-Hopf factorization, *IMA J. Appl. Math.*, *65*, 257–281, doi:10.1093/imamat/65.3.257.

Bart, H., I. Goheberg, and M. A. Kaashoek (1979), *Minimal Factorization of Matrix and Operator Functions*, Birkhuser Werlag, Basel, Switzerland.

Budaev, B. (1995), *Diffraction by Wedges*, Longman, New York.

Daniele, V. (1984), On the solution of vector Wiener-Hopf equations occurring in scattering problems, *Radio Sci.*, *19*, 1173–1178.

Daniele, V. (2003), The Wiener-Hopf technique for impenetrable wedges having arbitrary aperture angle, *SIAM J. Appl. Math.*, *63*, 1442–1460, doi:10.1137/S0036139901400239.

Daniele, V. (2004), An introduction to the Wiener-Hopf technique for the solution of electromagnetic problems, *Int. Rep. ELT-2004-1*, Politec. di Torino, Torina, Italy. (Available at http://www.eln.polito.it/staff/daniele.)

Daniele, V., and G. Lombardi (2006), Wiener-Hopf solution for impenetrable wedges at skew incidence, *IEEE Trans. Antennas Propag.*, *AP-54*, 2472–2485, doi:10.1109/TAP.2006.880723.

Gohberg, I. C., and M. G. Krein (1960), Systems of integral equation on a half line with kernels depending on the difference of arguments, *Trans. Am. Math. Soc., Ser. 2*, *14*, 217–287.

Gohberg, I. C., and N. Krupnik (1992), *One-Dimensional Linear Singular Integral Equation*, vol. 1, Birkhäuser, Boston.

Hashimoto, M., M. Idemen, and O. A. Tretyakov (1993), *Analytical and Numerical Methods in Electromagnetic Wave Theory*, Science House, Tokyo.

Jones, D. S. (1979), *Methods in Electromagnetic Wave Propagation*, Clarendon, Oxford, U. K.

Kantorovich, L. V., and V. I. Krylov (1958), *Approximate Methods of Higher Analysis*, P. Noordhoff, Groningen, Netherlands.

Lyalinov, M. A., and N. Y. Zhu (2005), Diffraction of a skew incident plane electromagnetic wave by a wedge with axially anisotropic impedance faces, paper presented at 28th URSI General Assembly, Int. Union of Radio Sci., New Delhi, India.

Noble, B. (1988), *Methods Based on the Wiener-Hopf Technique*, Chelsea, New York.

Vekua, N. P. (1967), *Systems of Singular Integral Equations*, P. Noordhoff, Groningen, Netherlands.

Weinstein, L. A. (1969), *The Theory of Diffraction and the Factorization Method*, Golem, Boulder, Colo.

Zhu, N. Y., and M. A. Lyalinov (2004), Diffraction of a normally incident plane wave by an impedance wedge with its exterior bisected by a semi-infinite impedance sheet, *IEEE Trans. Antennas Propag.*, *AP-52*, 2753–2758.

V. Daniele and G. Lombardi, Dipartimento di Elettronica, Politecnico di Torino, C. so Duca degli Abruzzi 24, I-10129 Torino, Italy. (vito.daniele@polito.it; guido.lombardi@polito.it)